

See discussions, stats, and author profiles for this publication at: <https://www.researchgate.net/publication/230382640>

A Consideration of the Application of Koutecký-Levich Plots in the Diagnoses of Charge-Transfer Mechanisms at Rotated Disk Electrodes

ARTICLE *in* ELECTROANALYSIS · FEBRUARY 2002

Impact Factor: 2.14 · DOI: 10.1002/1521-4109(200202)14:3<165::AID-ELAN165>3.0.CO;2-6

CITATIONS

63

READS

99

3 AUTHORS, INCLUDING:



Stephen Treimer

University of Iowa

12 PUBLICATIONS 207 CITATIONS

SEE PROFILE

Review

A Consideration of the Application of Koutecký-Levich Plots in the Diagnoses of Charge-Transfer Mechanisms at Rotated Disk Electrodes

Stephen Treimer, Andrew Tang^a, and Dennis C. Johnson*

Department of Chemistry and Ames Laboratory^b, Iowa State University, Ames, Iowa 50011, USA; email: dcj@iastate.edu.

^a Present Address: PC+ Computers, 108-5th St., Ames, IA 50011-3111, USA.

^b Ames Laboratory is operated for the U.S. Department of Energy by Iowa State University under Contract W-7405-Eng-82

Received: April 30, 2001

Final version: June 12, 2001

Abstract

It has become common practice to estimate the numbers of electrons (n , eq mol⁻¹) transferred in faradaic reactions at rotated disk electrodes (RDEs) from the slope of plots of reciprocal current ($1/I$) vs. reciprocal square root of rotational velocity ($1/\omega^{1/2}$). This practice is based on the Koutecký-Levich equation derived for a one-step electron-transfer mechanism. Furthermore, the intercept of the Koutecký-Levich plot is assumed to be a reciprocal function of the heterogeneous rate constant (k_h , cm s⁻¹) for the electron-transfer process. In this review, we examine the validity of the practice of estimating values of n and k_h for various multi-step mechanisms at RDEs.

Keywords: Koutecký-Levich equation and plots, Charge-transfer mechanisms, Rotating disk electrodes

1. Introduction

1.1. Rotated Disk Electrodes (RDEs) [1–7]

Applications of rotated disk electrodes (RDEs) to studies of electrode kinetics and mechanisms are documented [1–7]. Advantages of RDEs include: i) The rate of mass transport of reactants to a RDE surface is controlled precisely by fixing the rotational velocity (ω) of the electrode. ii) Electrode currents (I) quickly achieve steady-state values ($\partial I/\partial t = 0$) following establishment of applied electrode potential (E_{app}) for moderate-to-high rates of rotational velocity ($\omega > \text{ca. } 10 \text{ rad s}^{-1}$). As a consequence, voltammetric response ($I - E_{app}$) for a species transported from the bulk solution to the RDE surface is independent of potential scan rate for low rates of scan ($\phi < \text{ca. } 0.1 \text{ V s}^{-1}$). iii) Current response at RDEs is insensitive to incidental vibrations of the apparatus.

1.2. The Levich Response [1–7]

Consider the simple cathodic mechanism:



At steady-state, the rates of diffusional and convective transport of A are equal at the electrode surface and expressed:

$$D_A \left(\frac{\partial^2 C_A}{\partial x^2} \right)_{x=0} = v_x \left(\frac{\partial C_A}{\partial x} \right)_{x=0} \quad (2)$$

In Equation 2, v_x is the axial velocity of the solution at the electrode surface ($x \approx 0$) given approximately by the first two terms of a power series:

$$v_x = -0.510\omega^{3/2}\nu^{-1/2}x^2 + 0.333\omega^2\nu^{-1}x^3 \quad (3)$$

where ν is the kinematic viscosity of the solution (cm² s⁻¹). The second term in Equation 3 is frequently ignored for solutions of electroactive species having low diffusivity [1–7].

The cathodic electrode current (I_c) for the reduction of the oxidized species (A) to its reduced form (B) is written:

$$I_c = nF\pi r^2 D_A \left(\frac{\partial C_A}{\partial x} \right)_{x=0} = nF\pi r^2 D_A \left(\frac{C_A^b - C_A^s}{\delta} \right) \quad (4)$$

where n is the number of electrons transferred (eq mol⁻¹), F is the Faraday constant (96,487 C eq⁻¹), πr^2 is the geometric disc area (cm²) and C_A^s is the concentration of A at the electrode surface ($x = 0$). Also, in Equation 4, δ represents the thickness of the diffusion layer at the electrode surface and is defined by Equation 5 for species having low diffusivity.

$$\delta = [0.620]^{-1} D_A^{1/3} \nu^{1/6} \omega^{-1/2} \quad (5)$$

For large negative applied overpotential ($\eta = E_{app} - E^0 \ll 0$), $C_A^s \rightarrow 0$ and the cathodic response corresponds to that value limited by the maximum rate of convective-diffusional mass transport, as predicted by the so-called *Levich equation* for reactant species having low diffusivity [1].

$$I_{lim,c} = 0.620nF\pi r^2 D_A^{2/3} \nu^{-1/6} \omega^{1/2} C_A^b \quad (6)$$

For species having high diffusivity, the form of the *Levich equation* recommended by Gregory and Riddiford [6] is given by Equation 7; see especially p. 365 of [7].

$$I_{\text{lim},c} = \left[\frac{0.554}{0.893 + 0.316(D/v)^{0.36}} \right] nF\pi r^2 D_A^{2/3} v^{-1/6} \omega^{1/2} C_A^b \quad (7)$$

Accordingly, for reactant species having high diffusivity, the thickness of the diffusion layer is given by:

$$\delta = \left[\frac{0.554}{0.893 + 0.316(D/v)^{0.36}} \right]^{-1} D_A^{1/3} v^{1/6} \omega^{-1/2} \quad (8)$$

Evidence that an electrode response corresponds to Equations 6 and/or 7 is the observation of a linear dependence of $I_{\text{lim},c}$ on the product $\omega^{1/2} C_A^b$.

In the remainder of this review, reactant species will be considered to have low diffusivity, i.e., Equations 5 and 6 are assumed to define δ and $I_{\text{lim},c}$.

1.3. Voltammetric Principles

For small values of η in a solution of A, having fast electron transfer, C_A^s is defined:

$$C_A^s = C_A^b \exp\{\theta\} \quad (9)$$

where $\theta = nF\eta/RT$. The electrode current can then expressed:

$$I_c = \frac{nF\pi r^2 D_A C_A^b}{\delta[1 + \exp\{\theta\}]} \quad (10)$$

Plots of I_c vs. $\omega^{1/2}$ are predicted to be linear at all η with slopes proportional to n . At $\eta = 0$, i.e., $E_{\text{app}} = E^0$, $\exp\{\theta\} = 1$ and $I_c = 0.5 I_{\text{lim},c}$. For $\theta \ll 0$, $\exp\{\theta\} \approx 0$ and $I_c = I_{\text{lim},c}$.

1.4. The Koutecký-Levich Response [9]

Equation 6 is the ideal response of fast electron-transfer processes. For systems with slow electron transfer, the electrode current is defined:

$$I_c = nF\pi r^2 k_h C_A^s \quad (11)$$

where k_h (cm s⁻¹) is the heterogeneous rate constant for electron transfer.

$$k_h = k_0 \exp\left[\frac{-\alpha F\eta}{RT}\right] \quad (12)$$

As predicted by Equation 11, $C_A^s \rightarrow C_A^b$ for $k_h \rightarrow 0$ and $C_A^s \rightarrow 0$ for $k_h \rightarrow \infty$.

Of greatest importance for this review are examples of reactions for which the rates of mass transport and electron transfer are comparable and $0 < C_A^s < C_A^b$. These cases are described as having *mixed transport-kinetic control*. The electrode current for such cases is then described by both Equations 4 and 11. Combining these equations to eliminate C_A^s and solving for I_c produces the so-called *Koutecký-Levich equation* [8].

$$I_c = \frac{nF\pi r^2 D_A C_A^b}{\delta + D_A/k_h} \quad (13)$$

The functionally useful form of Equation 13 is the reciprocal of I_c , given by:

$$\frac{1}{I_c} = \frac{\delta}{nF\pi r^2 D_A C_A^b} + \frac{1}{nF\pi r^2 k_h C_A^b} \quad (14)$$

Substituting Equation 5 into Equation 14 yields:

$$\frac{1}{I_c} = \frac{1}{0.62 nF\pi r^2 D_A^{2/3} v^{-1/6} \omega^{1/2} C_A^b} + \frac{1}{nF\pi r^2 k_h C_A^b} \quad (15)$$

Hence, for cathodic reactions governed by mixed transport-kinetic control, plots of $1/I_c$ vs. $1/\omega^{1/2}$ for constant values of k_h , i.e., fixed η , are predicted to generate straight lines having slopes proportional to $1/n$ and intercepts proportional to $1/k_h$. It is important to observe that the slopes of these plots are independent of applied overpotential.

It is tempting to apply Equation 16 for the analyses of all amperometric and voltammetric data to determine values for n and k_h . Indeed, this action appears viable when experimental plots of $1/I_c$ vs. $1/\omega^{1/2}$ exhibit linearity. This review examines the nature of $1/I_c$ vs. $1/\omega^{1/2}$ plots predicted for various mechanisms at RDEs.

1.5. Multi-Step Mechanisms

In the discussion below, electron-transfer and chemical steps are represented by symbols **E** and **C**, respectively. Furthermore, subscripts **r** and **i** qualify the steps as being *reversible* (kinetically fast) or *irreversible* (kinetically slow), respectively. Hence, a **C_iE_i** designation implies an irreversible chemical step followed by an irreversible electron-transfer step.

It also is assumed that all steps in the mechanism proceed at comparable rates or that one step is slow, i.e., the rate determining step (rds). For example, in an **EC** mechanism, the **E** step is assumed to be fast, else the **C** step does not proceed significantly and the mechanism exhibits the characteristics of a single **E** step. It is also assumed that all species in solution have equal values of diffusion coefficient (*D*).

2. EE Mechanisms [9, 10]

Consider a cathodic mechanism involving two consecutive one-electron steps, i.e., an **EE** mechanism, as represented by:



In deriving equations for the net cathodic electrode current, it is assumed that the first step is at equilibrium, $E_1^{0'} > E_2^{0'}$, and the diffusion coefficients for all species are identical [9]. Furthermore, in this mechanism, any reaction between the reactant and the product, i.e., comproportionation, is assumed negligible. Sakai et al. present a nice treatment for the current response at an RRDE due to an **EE** mechanism [10].

2.1. Special Case of $E_r E_r$

The current for the $E_r E_r$ mechanism is given by:

$$I_c = \frac{F\pi r^2 D_A C_A^b}{\delta} \left[2 - \frac{\exp\{\theta_2\} + 2\exp\{\theta_1 + \theta_2\}}{1 + \exp\{\theta_2\} + \exp\{\theta_1 + \theta_2\}} \right] \quad (18)$$

where $\theta_1 = F\eta_1/RT$ and $\theta_2 = F\eta_2/RT$. Taking the reciprocal, Equation 18 becomes:

$$\frac{1}{I_c} = \frac{\delta}{F\pi r^2 D_A C_A^b} \left[\frac{1 + \exp\{\theta_2\} + \exp\{\theta_1 + \theta_2\}}{2 + \exp\{\theta_2\}} \right] \quad (19)$$

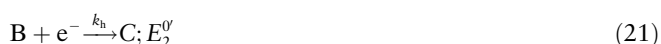
Accordingly, plots of $1/I_c$ vs. $1/\omega^{1/2}$ are expected to be linear with zero intercepts and slopes that vary as a function of applied overpotential. At very negative potentials ($E_2^{0'} \gg \eta$), the exponential terms in Equation 19 are negligible, and the current is limited by convective-diffusional transport, as described by:

$$\frac{1}{I_c} = \frac{1}{I_{\text{lim},c}} = \frac{1}{0.62nF\pi r^2 D_A^{2/3} \nu^{-1/6} \omega^{1/2} C_A^b} \quad (20)$$

Only in the case where $E_2^{0'} \gg \eta$ is the slope of the reciprocal plot a reliable measure of the total value of n for the sequential processes.

2.2 Special Case of $E_r E_i$

The second step in the $E_r E_i$ mechanism is denoted:



The electrode current for an $E_r E_i$ mechanism is defined:

$$I_c = \frac{F\pi r^2 D_A C_A^b}{\delta} \left[2 - \frac{D_A [2\exp\{\theta_1\} + 1]}{\delta k_h + D_A [\exp\{\theta_1\} + 1]} \right] \quad (22)$$

$$= \frac{F\pi r^2 D_A C_A^b}{\delta} \left[\frac{D_A + 2\delta k_h}{\delta k_h + D_A [\exp\{\theta_1\} + 1]} \right]$$

According to Equation 22, the apparent value of n approaches 2 eq mol⁻¹ for $\delta k_h \rightarrow 0$, i.e., large negative overpotential. This is equivalent to a convective-diffusional transport-limited reaction with $n = 2$ eq mol⁻¹. Written in reciprocal form, Equation 22 becomes:

$$\frac{1}{I_c} = \frac{\delta}{F\pi r^2 D_A C_A^b} \left[\frac{\delta k_h + D_A [\exp\{\theta_1\} + 1]}{D_A + 2\delta k_h} \right] \quad (23)$$

There are two limiting cases for Equation 23: i) For $E_{\text{app}} > E_2$, the second step is slow. This corresponds to $D_A \gg 2\delta k_h$, and the current is the same as for E_r and is given by Equation 20. ii) When $E_{\text{app}} < E_2$, the second step is fast. This corresponds to $D_A \ll 2\delta k_h$, and the reciprocal current is given by:

$$\frac{1}{I_c} = \frac{\delta}{2F\pi r^2 D_A C_A^b} + \frac{\exp\{\theta_1\}}{2F\pi r^2 k_h C_A^b} \quad (24)$$

Hence, for the $E_r E_i$ mechanism, plots of $1/I_c$ vs. $1/\omega^{1/2}$ exhibit a slope inversely proportional to the total number of electrons passed in the step-wise mechanism ($1/n_{\text{tot}}$) and an intercept inversely proportional to the heterogeneous rate constant for the second irreversible step ($1/k_h$). From this, we conclude that, for a multi-stepwise mechanism, the apparent number of electrons (n_{app}) determined from the plot of $1/I_c$ vs. $1/\omega^{1/2}$ corresponds to the sum of the electrons passed for the fast steps plus the rate determining step. Clearly, this value of n_{app} can be equal to or less than the total number of electrons (n_{tot}) determined from the coulometric result of exhaustive electrolysis.

3. Introduction to EC and CE Mechanisms [11, 12]

It is common to have chemical reactions occurring in solution before, after or between electron transfer steps. The mathematical analyses of these mechanisms are simplified by the use of the reaction layer approach [12, 13], the principle of which is illustrated by the following example. For an **EC** reaction scheme, we write:



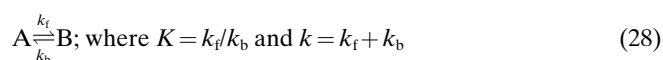
The formation of C from B is assumed to be complete within a reaction layer at the electrode surface having a thickness of μ defined by:

$$\mu = (D_B/k)^{1/2} \quad (27)$$

A small μ corresponds to a very short lifetime of B ($k \gg 0$), e.g., for $\mu \ll \delta$, the contribution from convection can be ignored and the problem is reduced to a diffusion-controlled process modified by a chemical reaction. The reaction layer thickness is also viewed as a parameter that emerges through the solution of the equations describing the electrochemical-chemical system [13], where k is a linear combination of the rate constants of the chemical step.

4. CE Mechanisms [14–16]

Initial interpretations of **CE** mechanisms were made by Koutecký and Levich [13]. Further contributions were offered by Alberly [14], Compton et al. [15], Rebouillat et al. [16]. For the electroinactive species A in equilibrium with the electroactive B species, the first step in the **CE** mechanism is represented by:



Several unique versions of **CE** mechanism exist, and are presented below.

4.1. Case of $C_r E_r$

The second step is represented by:



For the situation, the electrode current is given by:

$$I_c = \frac{nF\pi r^2 D_B K C^b}{\delta[K + (1 + K) \exp\{\theta_1\}] + \mu} \quad (30)$$

where $C^b = C_A^b + C_B^b$. Equation 30 is accurate when $(D_B/v)^{1/3} \ll k/\omega$. When $K \gg 1$, $I_c = I_{\text{lim},c}$. Equation 30 can be rearranged to:

$$\frac{1}{I_c} = \frac{\delta[K + (1 + K) \exp\{\theta_1\}]}{nF\pi r^2 D_B K C^b} + \frac{\mu}{nF\pi r^2 K D_B C^b} \quad (31)$$

According to Equation 31, plots of $1/I_c$ vs. $1/\omega^{1/2}$ are predicted to be linear with intercepts proportional to μ/K . Again, it is important to note that the slopes of reciprocal plots for this mechanism are a function of applied overpotential.

4.2. Case of $C_r E_i$

The second step is represented by:



The current is given by:

$$I_c = \frac{nF\pi r^2 D_B K k_h C^b}{D_B(1 + K) + k_h(\mu + \delta K)} \quad (33)$$

which, in the reciprocal form, is written:

$$\frac{1}{I_c} = \frac{\delta}{nF\pi r^2 D_B C^b} + \frac{D_B(1 + K) + \mu k_h}{nF\pi r^2 D_B K k_h C^b} \quad (34)$$

For this mechanism, the slopes of reciprocal plots are not a function of applied overpotential.

5. EC Mechanisms [17–21]

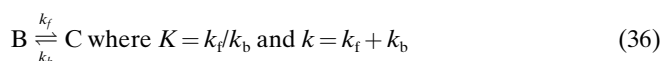
Galus [17] first made observations of the **EC** mechanism represented by:



in which species B is converted to an electroinactive species C via a chemical process. Bard and Faulkner have provided a general overview of **EC** processes at RDEs [18].

5.1. Case of $E_r C_r$

The chemical step is reversible, as represented by:



The current is given by the expression:

$$I_c = \frac{nF\pi r^2 D_A (1 + K) C_A^b}{\delta[1 + K + \exp\{\theta_1\}] + \mu K \exp\{\theta_1\}} \quad (37)$$

with the reciprocal being written:

$$\frac{1}{I_c} = \frac{\delta[1 + K + \exp\{\theta_1\}]}{nF\pi r^2 D_A (1 + K) C_A^b} + \frac{\mu K \exp\{\theta_1\}}{nF\pi r^2 D_A (1 + K) C_A^b} \quad (38)$$

For this mechanism, slopes of the reciprocal plots are a function of applied overpotential.

5.2. Case of $E_r C_i$

The second step is irreversible, as represented by:



The current for which is:

$$I_c = \frac{nF\pi r^2 D_A C_A^b}{\delta + \mu \exp\{\theta_1\}} \quad (40)$$

which, in the reciprocal form, is given by:

$$\frac{1}{I_c} = \frac{\delta}{nF\pi r^2 D_A C_A^b} + \frac{\mu \exp\{\theta_1\}}{nF\pi r^2 D_A C_A^b} \quad (41)$$

This expression is reasonably accurate for values of $\delta/\mu > 50$. As noted in Equation 41, slopes of the reciprocal plots are not a function of applied overpotential.

5.3. EC_i' Mechanisms

McIntyre et al. [19] elucidated the EC_i' mechanism. Compton and co-workers have contributed significant recent interpretations for the EC_i' mechanism [20, 21]. The reactant is regenerated from the product by a chemical step, considered to be *catalytic*, as indicated by:



The current is given by:

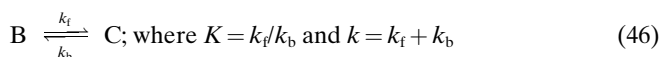
$$I_c = \frac{nF\pi r^2 D_A C_A^b}{\mu[1 + \exp\{\theta_1\}]} \quad (44)$$

For this mechanism, $I_{\text{lim},c} = nF\theta r^2(D_A/\mu) C_A^b$ at $\theta \ll 0$.

It is apparent from Equation 44 that the current observed for EC_i' is a factor of δ/μ times the current due solely to mass transport and is independent of the rotational speed. This conclusion assumes k_f is large compared to D_A/δ and, hence, the effect of mass transport is negligible. When this assumption is no longer valid, the observed current has both mass transport and catalytic components. The observed current approaches the transport-limited current for the A species in the bulk solution as the rotational velocity is increased. In general, for EC_i' mechanisms, plots of I_c vs. $\omega^{1/2}$ have non-zero intercepts. The EC_i' mechanism at chemically modified electrodes, though well documented in the literature, will not be interpreted by this work due to complications arising from the interpretations of Michaelis-Menten style kinetics.

6. ECE Mechanism [22–24]

Filinovskii, made some of the early predictions for various **ECE** mechanisms [2]. Subsequent work by Amatore and co-workers [22, 23] and Compton et al. [24] further developed the theoretical model for the **ECE** mechanism. In a cathodic **ECE** mechanism, the reactant (A) is reduced to the electroinactive species B via electron-transfer. The species B is chemically transformed in solution to an electroactive intermediate (C) which undergoes further reduction to give the final product (D). The three steps in the **ECE** mechanism are represented by:



6.1. Case of $\text{E}_r\text{C}_r\text{E}_r$

The cathodic current for this sequential mechanism is given by:

$$I_c = \frac{2F\pi r^2 D_A K C_A^b}{\delta K + \mu(1 + K) \exp\{\theta_1\} + \delta \exp\{\theta_1 + \theta_2\}} \quad (48)$$

Rearranging to the reciprocal form, gives:

$$\frac{1}{I_c} = \frac{\delta[K + \exp\{\theta_1 + \theta_2\}]}{2F\pi r^2 D_A K C_A^b} + \frac{\mu(1 + K) + \exp\{\theta_1\}}{2F\pi r^2 D_A K C_A^b} \quad (49)$$

Again, it is important to note that the slopes of reciprocal plots for this mechanism are a function of applied overpotential.

6.2. Case of $\text{E}_r\text{C}_r\text{E}_i$

For such a mechanism, the third step corresponds to:



with the current denoted:

$$I_c = \frac{2F\pi r^2 D_A K k_h C_A^b}{\delta K k_h + [D_A + \mu(1 + K) k_h] \exp\{\theta_1\}} \quad (51)$$

Rearranging to the reciprocal form, we get:

$$\frac{1}{I_c} = \frac{\delta}{2F\pi r^2 D_A C_A^b} + \frac{[D_A + \mu(1 + K) k_h] \exp\{\theta_1\}}{2F\pi r^2 D_A K k_h C_A^b} \quad (52)$$

The slopes of reciprocal plots for this mechanism are not a function of applied potential.

7. Partially Blocked Electrodes [25–33]

The preceding treatments assume that the electrode surfaces are uniformly active and accessible to the reactants. Landsberg, Scheller, and co-workers brought to light significant advances in *blocked* or *inhomogeneous* electrodes; electrodes that are not fully accessible to solution [25–27], possibly the result of the formation of an inert organic film, oxide, adsorbed gas bubbles, or insufficiently clean surface preparation. There are two types of inhomogeneous electrodes: *macroscopic* [28, 29] is when the size of active regions and the distance between them are similar to the thickness of the diffusion layer; and *microscopic* [30, 31] is when the size of the active regions and the distance between them are much smaller than the thickness of the diffusion layer.

Useful treatments for the diagnosis of mechanisms at polymer coated rotated disc electrodes using Koutecký-Levich plots have been developed recently, but will not be presented in this brief article.

7.1. Macroscopic Inhomogeneity

The response of an inhomogeneous electrode is complicated by radial (nonlinear) diffusion and convection mass transport. Let f denote the fraction of the surface that is inactive. For an inhomogeneous RDE with $f=0.5$, Levart [32] compared digital simulations of the effect of the radius of the active sites (r_s) on the ratio (ρ) of the observed currents to the transport-limited currents for a fully active RDE. For these simulations, the diameter of the active sites was set equal to distance between these sites. For $r_s > 10 \delta$, ρ was independent of δ . At $r_s > \delta$, ρ increased with increasing δ . Because ρ depends on δ , the $I - \omega^{1/2}$ plot exhibited a reaction under mixed transport-kinetic control. Over the range $0.96 \geq f \geq 0.50$, ρ was greater than $1-f$, i.e., the current was larger than expected if the total active area behaved as one contiguous surface. The additional current was due to the contribution of radial convection to mass transport.

Radial diffusion is most significant at small electrodes and low rotation speeds. Landsberg and co-workers [25] offered an analytical approach to the current response due to radial convection, further refined by Scheller and co-workers [26, 27], and summarized by Filinovskii and Pleskov [2, 3]. According to the model, active sites were circular with radius r_1 , uniformly distributed on the electrode surface, and concentric with one end of a larger, imaginary cylinder. Mass transfer between the sites and the solution occurred by diffusion inside the cylinders, each with length δ and radius r_2 . Given $\delta \gg r_2$, the model predicted linear plots of $1/I$ vs. $1/\omega^{1/2}$, with intercepts as Bessel functions of the quantity r_1/r_2 . This case has been experimentally verified [25–27]. For $\delta \ll r_2$, a plot of I vs. $\omega^{1/2}$ was linear with slope as a different Bessel function of r_1/r_2 , less than the Levich slope. The model was not very realistic because each site would have its own diffusion layer [28], but gave the correct functional dependence [26]. Caprani and Frayret [33] developed an Equation for a partially blocked surface with independently active sites, for which the current is summed for each micro-electrode over the entire surface. The Equation is:

$$\rho = 1.1 \pi r^{1/3} (1-f)^{5/6} d^{1/6} \quad (53)$$

where r is the radius of the RDE and d is the number of active sites per unit of geometric area.

7.2. Microscopic Inhomogeneity

Amatore et al. proposed two sub-cases for diffusion to microscopically inhomogeneous surfaces [30]. First, when $f \ll 1$, the standard rate constant for electron transfer is $(1-f)$ times that of the standard rate constant for a fully active

electrode. Second, for $f \approx 1$, the amount of reactant electrolyzed is sufficiently low relative to the rate of diffusion, therefore the concentration near the electrode reaches a steady state and the voltammetric response obtained for a quiescent solution has the appearance of the response obtained in stirred solution. The limiting current is given by:

$$I_{\text{lim}} = \frac{F\pi r^2 D_A C_A^b}{2r_o \Phi(1-f)} \quad (54)$$

where $\Phi(1-f)$ is $0.3(1-f)^{-1/2}$ for disk type sites and $1 - (1/\pi) \ln \sin\{(\pi/2)(1-f)\}$ for stripe-type sites and $2r_o$ is the distance between the centers of two adjacent sites.

Although the results of Amatore et al. were derived for diffusion to stationary electrodes, they should apply for RDE systems if $\delta \gg 2r_o$. Therefore a microscopically inhomogeneous RDE with $f \ll 1$ is equivalent to a fully active electrode of the same geometry with a slower electron transfer rate at the same applied potential. When $f \rightarrow 1$, the current is not a function of rotational speed and is not necessarily smaller than the diffusion-limited current at a geometrically identical, fully active electrode.

8. Diagnosis of Mechanisms

The primary motivation in many electroanalytical studies of electrode response at hydrodynamic electrodes is the determination of the value for n (eq mol⁻¹) corresponding to the charge-transfer component of the response mechanism. A secondary objective is identification of the simplest mechanism that is consistent with observed variations in electrode response as a function of changes in the rate of convective-diffusional mass transport. And, of course, associated with this mechanistic diagnosis is the evaluation of the rate constant corresponding to the rate-determining step (rds).

Linearity of Levich plots of I vs. $\omega^{1/2}$ over an extended range of ω values, e.g., 5–1000 rad s⁻¹ (50–10000 rev min⁻¹), is indicative of a response mechanism that can be approximated as a single step resulting in the rapid transfer of n electrons characterized by a large heterogeneous rate constant (k_h). For this case, the n value can be reliably estimated from the slope using literature values of v and D . If these values are not available, the estimation $v = 1.0 \times 10^{-2}$ cm² s⁻¹ is useful for most aqueous media and $D = 1.0 \times 10^{-5}$ cm² s⁻¹ is a common approximation for small reactant species in aqueous media. Negative curvature in plots of I vs. $\omega^{1/2}$ can be indicative of slow charge-transfer kinetics, as indicated by Equation 10. Of course, this is the mechanism presumed in the derivation of the Koutecký-Levich equation and, therefore, the plot of $1/I$ vs. $1/\omega^{1/2}$ is recommended. Accordingly, we recommend estimation of n values from both the linear segment of the Levich plot at low ω values (< ca. 100 rad s⁻¹) and from the linear segment of the Koutecký-Levich plot at large ω values (> ca. 100 rad s⁻¹). Equality of these two n values can be interpreted as confirmation of the diagnosis of a one-step mechanism

involving the transfer of n electrons with a moderately slow heterogeneous rate constant (k_h). Furthermore, k_h can be evaluated from the non-zero intercept of the Koutecký-Levich plot, as indicated by Equation 15.

Should one observe that the value of n calculated from the Levich plot for low ω values is larger than that estimated from the Koutecký-Levich plot for large ω values can be interpreted as indicative of two or more consecutive charge transfer steps, e.g., E_rE_i and E_rCE_i mechanisms, wherein the second charge-transfer step occurs with a k_h value much smaller than that for the first charge-transfer step. It can be helpful in such cases to determine an overall n value from coulometric results for an exhaustive electrolysis.

Partially blocked electrode surfaces usually are the undesired consequence of the adsorption of organic impurities from the bulk solution and/or the polymerization of free-radical intermediate products of incomplete electrode reactions involving organic reactants. Therefore, electrode response under these situations will demonstrate a steady decay with continued use. Electrode response can be restored by mechanical polishing, sonication, and/or application of positive-negative potential steps to cause anodic or cathodic desorption of the films [34–37].

Finally, apply different electrode geometries and/or chronoamperometry and the corresponding theories to elucidate ambiguous results of the RDE voltammetry to assist in the unambiguous determination of the mechanism [38].

9. References

- [1] V. G. Levich, *Physicochemical Hydrodynamics*, 2nd. ed., Prentice-Hall, Englewood Cliffs, N. J., **1962**, pp. 60–72.
- [2] Y. V. Pleskov, V. Y. Filinovskii, *The Rotating Disc Electrode* (Ed: H. S. Wroblowa) Consultants Bureau, New York **1976**, ch. 2.
- [3] V. Y. Filinovskii, Y. V. Pleskov, *Progress in Surface and Membrane Science*, Vol. 10 (Eds: D. A. Cadenhead, J. F. Danielli), Academic Press, New York **1976**, p. 27.
- [4] Z. Galus, *Fundamental of Electrochemical Analysis* (Ed: S. Marcinkiewicz), Halsted, New York **1976**.
- [5] A. J. Bard, L. R. Faulkner, *Electrochemical Methods*, 1st ed., Wiley, New York **1980**, ch. 8.
- [6] D. P. Gregory, A. C. Riddiford, *J. Chem. Soc.* **1956**, 3756.
- [7] C. M. A. Brett, A. M. Oliveira Brett, *Comprehensive Chemical Kinetics*, Vol. 26 (Ed: C. H. Bamford, R. G. Compton), Elsevier, Amsterdam **1986**, ch. 5.
- [8] J. Koutecký, V. G. Levich, *Zh. Fiz. Khim.* **1956**, 32, 1565.
- [9] Z. Rongfeng, D. H. Evans, *J. Electroanal. Chem.* **1995**, 385, 201.
- [10] M. Sakai, N. Ohnaka, *J. Electrochem. Soc.* **1990**, 137, 576.
- [11] J. Koutecký, R. Brdicka, *Coll. Czech. Chem. Comm.* **1947**, 12, 337.
- [12] P. Delahay, *New Instrumental Methods in Electrochemistry*, Wiley-Interscience, New York **1954**, p. 92.
- [13] J. Koutecký, V. G. Levich, *Dokl. Akad. Nauk. SSSR* **1957**, 117, 441.
- [14] W. J. Albery, *Electrode Kinetics*, Clarendon Press, Oxford **1975**, ch. 5.
- [15] R. G. Compton, R. G. Harland, *J. Chem. Soc., Faraday Trans. 1*, **1989**, 85, 761.
- [16] S. Rebouillat, M. E. G. Lyons, T. Bannon, *J. Solid State Electrochem.* **1999**, 3, 215.
- [17] Z. Galus, R. N. Adams, *J. Electroanal. Chem.* **1962**, 4, 248.
- [18] A. Bard, L. Faulkner, *Electrochemical Methods*, 1st ed., Wiley, New York **1980**, p. 466.
- [19] J. D. E. McIntyre, *J. Phys. Chem.* **1967**, 71, 1196.
- [20] R. G. Compton, M. J. Day, M. E. Laing, R. J. Northing, J. I. Penman, A. M. Waller, *J. Chem. Soc., Faraday Trans. 1*, **1988**, 84, 2013.
- [21] R. G. Compton, R. A. Spackman, P. R. Unwin, *J. Electroanal. Chem.* **1989**, 264, 1.
- [22] C. Amatore, J.-M. Savéant, *J. Electroanal. Chem.* **1977**, 85, 27.
- [23] C. Amatore, M. Gareil, J.-M. Savéant, *J. Electroanal. Chem.* **1983**, 147, 1.
- [24] R. G. Compton, R. G. Harland, P. R. Unwin, A. M. Waller, *J. Chem. Soc., Faraday Trans. 1*, **1987**, 83, 1261.
- [25] R. Landsberg, R. Thiele, *Electrochim. Acta* **1966**, 11, 1243.
- [26] F. Scheller, S. Müller, R. Landsberg, H.-J. Spitzer, *J. Electroanal. Chem.* **1968**, 19, 187.
- [27] F. Scheller, R. Landsberg, S. Müller, *J. Electroanal. Chem.* **1969**, 20, 375.
- [28] Y. M. Povarov, P. D. Lukovtsev, *Electrochim. Acta* **1973**, 18, 13.
- [29] V. Y. Filinovskii, *Electrochim. Acta* **1980**, 25, 309.
- [30] C. Amatore, J.-M. Savéant, D. Tessier, *J. Electroanal. Chem. Interfacial Electrochem.* **1983**, 147, 39.
- [31] O. Contamin, E. Levart, *J. Electroanal. Chem.* **1982**, 136, 259.
- [32] E. Levart, *J. Electroanal. Chem.* **1985**, 187, 247.
- [33] A. Caprani, J. P. Frayret, *J. Electroanal. Chem.* **1982**, 138, 155.
- [34] D. C. Johnson, W. R. LaCourse, *Anal. Chem.* **1990**, 62, 589A.
- [35] W. R. LaCourse, D. C. Johnson, in *Advances in Ion Chromatography*, Vol. 2 (Eds: P. Jandik, R. M. Cassidy), Century International, Medfield, MA **1990** 353.
- [36] W. R. LaCourse, *Pulsed Electrochemical Detection in High-Performance Liquid Chromatography*, Wiley, New York **1997**.
- [37] S. Ranganathan, T.-C. Kuo, R. L. McCreery, *Anal. Chem.* **1999**, 71, 3574.
- [38] R. G. Compton, M. E. Laing, D. Mason, R. J. Northing, P. R. Unwin, *Proc. R. Soc. London A* **1988**, 418, 113.